1   # Cellular correlates of cortical thinning throughout the lifespan

2   ## Lifespan cellular correlates of cortical thinning

3

4   Vidal-Pineiro, D. PhD[1], Parker, N., M.Sc.[2,3], Shin, J. PhD[4], French, L. PhD[5], Grydeland, H. PhD[1],

5   Jackowski, AP. MD/PhD[6,7], Mowinckel, AM. PhD[1], Patel, Y.[2,3], Pausova, Z., MD[4], Salum, G. MD/PhD[7,8],

6   Sørensen, Ø., PhD[1], Walhovd, KB PhD[1,9], Paus, T., MD/PhD[2,3,10]*, Fjell, AM PhD[1,9]*, for the

7   Alzheimer's Disease Neuroimaging Initiative, for the Australian Imaging Biomarkers[&] and Lifestyle

8   flagship study of ageing[Δ]

9

10   [1]Centre for Lifespan Changes in Brain and Cognition, Department of Psychology, University of Oslo,

11   Oslo, 0317, Norway.

12   [2]Bloorview Research Institute, Holland Bloorview Kids Rehabilitation Hospital, Toronto, ON, M4G

13   1R8, Canada;

14   [3]Institute of Medical Science, University of Toronto, Toronto, ON, M5S 1A8, Canada

15   [4]The Hospital for Sick Children, University of Toronto, Toronto, ON, M5G 1X8, Canada;

16   [5]Centre for Addiction and Mental Health, University of Toronto, Toronto, ON, M5T 1L8, Canada

17   [6]Interdisciplinary Lab for Clinical Neurosciences (LiNC), University Federal of São Paulo, 04038-020,

18   Brazil

19   [7]National Institute of Developmental Psychiatry for Children and Adolescents (INCT-CNPq), São

20   Paulo, 90035-003, Brazil

21   [8]Department of Psychiatry, Federal University of Rio Grande do Sul, Porto Alegre, 90035-003, Brazil

22   [9]Department of radiology and nuclear medicine, Oslo University Hospital, Oslo, 0450, Norway

23   [10]Departments of Psychology and Psychiatry, University of Toronto, ON, M5T 1R8, Canada

31   Industrial Research Organisation (CSIRO), which was made available at the ADNI database

32   (www.loni.usc.edu/ADNI). The AIBL researchers contributed data but did not participate in analysis

33   or writing of this report. AIBL researchers are listed at www.aibl.csiro.au.

34   *Denotes equal contribution and corresponding authors

35

36   **Corresponding authors:**

37

38   **Tomáš Paus**

39   Bloorview Research Institute, 150 Kilgour Road

40   Toronto, Ontario, Canada, M4G 1R8

41   tpaus@hollandbloorview.ca

42   Tel: (416) 425-6220, extension 6023

43   Fax: 416 525 6591

44

45   **Anders Martin Fjell**

46   Department of Psychology, Pb. 1094 Blindern

47   Oslo, Norway, 0317

48   a.m.fjell@psykologi.uio.no

49   Tel: (+47)-22845129

50   **Abstract**

51

52   Cortical thinning occurs throughout the entire life and extends to late-life neurodegeneration, yet

53   the neurobiological substrates are poorly understood. Here, we used a virtual-histology technique

54   and gene expression data from the Allen Human Brain Atlas to compare the regional profiles of

55   longitudinal cortical thinning through life (4004 MRIs) with those of gene expression for several

56   neuronal and non-neuronal cell types. The results were replicated in three independent longitudinal

57   datasets. We found that inter-regional profiles of cortical thinning related to expression profiles for

58   marker genes of CA1 pyramidal cells, astrocytes and microglia during development and in aging.

59   During the two stages of life, the relationships went in opposite directions: greater gene expression

60   related to less thinning in development and *vice versa* in aging. The association between cortical

61   thinning and cell-specific gene expression was also present in mild cognitive impairment and

62   Alzheimer's Disease. These findings suggest a role of astrocytes and microglia in promoting and

63   supporting neuronal growth and dendritic structures through life that affects cortical thickness

64   during development, aging, and neurodegeneration. Overall, the findings contribute to our

65   understanding of the neurobiology underlying variations in MRI-derived estimates of cortical

66   thinning through life and late-life disease.

Introduction

67

68

69 The human cerebral cortex undergoes constant remodeling throughout the lifespan. Magnetic

70 resonance imaging (MRI) enables the estimation of structural properties of the human cerebral

71 cortex that can, in turn, be related to cognitive, clinical and demographic data[1,2], used as biomarkers

72 of neurodegeneration[3,4] or as high-fidelity phenotypes for genomic studies[5,6]. Yet, we lack data for

73 guiding interpretation of MRI-based phenotypes with regard to the underlying neurobiology[8,9].

74 Relating MRI-based variations in cortical thickness to specific neurobiological processes is

75 fundamental for our understanding of the normal lifespan trajectories and individual differences in

76 cortical thickness, as well as the nature of cortical abnormalities in brain disorders and diseases such

77 as Alzheimer's Disease (AD). Here, we approach this question by studying the regional patterns of

78 age-related cortical thinning in relation to those of the expression of genes indexing several neuronal

79 and non-neuronal cell types.

80

81 For MRI-based estimates of cortical thickness, the prototypic lifespan-trajectory includes a steep

82 age-related decrease in childhood and adolescence, followed by a mild monotonic thinning from

83 early adulthood and, in many regions, an accelerated thinning from about the seventh decade of

84 life[10,11]. Despite uninterrupted cortical thinning during the lifespan, the underlying neurobiological

85 substrates and processes must be – at least partially - different. Developmental changes in cortical

86 thickness may involve processes such as intracortical myelination, remodeling of dendritic arbours

87 and its components (e.g., dendritic spines), axonal sprouting, and vascularization[12–15]. With

88 advancing age, cortical thinning may, for instance, be associated with neuronal and dendritic

89 shrinkage[16–18]. Cortical thinning in AD could be also influenced by the degree of neuronal loss[19].

90

91   The human cerebral cortex contains many types of cells, which can be classified into neuronal –

92   mostly pyramidal cells and interneurons - and non-neuronal cells - mostly glial cells, namely

93   microglia, astrocytes and oligodendrocytes[19–21]. Histological data suggest that regional variations of

94   cortical thickness may be associated with the number of non-neuronal cells and neuropil volume[23,24].

95   Yet, *ex vivo* approaches have limitations when it comes to understanding the cellular substrate

96   driving age-related changes in cortical thickness in the general population. Two studies have

97   addressed this issue by combining cross-sectional estimates of cortical thickness during adolescence

98   with quantitative MRI data and gene expression data[24,25]. By combining magnetization transfer and

99   cortical thickness estimates, Whitaker and colleagues[25] suggested intra-cortical myelination as a

100   primary driver of cortical thinning in the adolescent cortex. On the other side, Shin and colleagues[24]

101   combined regional profiles of age-related cortical thickness in adolescence and cell-specific gene

102   expression using the Allen Human Brain Atlas (AHBA)[27]. Their results suggested that – across the

103   cerebral cortex – inter-regional variations in cortical thinning are associated with inter-regional

104   variations in the expression of marker genes for CA1 pyramidal cells, astrocytes, and microglia

105   (regions with more expression showing less thinning).

106

107   It is, however, unclear to which degree cortical thinning relates to the same gene expression

108   patterns throughout development and aging. The answer to this question has implications for our

109   understanding of the neurobiological foundation for age-related changes in cortical thinning. Thus,

110   the main objective of the study was to shed light on the neurobiological substrates underlying

111   cortical thinning at different stages during the lifespan. Here we ask whether age-related changes in

112   thickness of the human cerebral cortex, assessed *in vivo* with longitudinal MRI, are associated with

113   specific neuronal or non-neuronal cell-types. We approached this question by correlating regional

114   profiles of cortical thinning – during different periods of the lifespan - with regional profiles of cell-

115   specific gene expression. We followed up the results with two supplementary questions: i) Is the

116   cortical thinning – gene expression relationship in young and older adults supported by one or

117   several neurobiological mechanisms? ii) Does the cortical thinning – gene expression relationship

118   extend into to the aging-dementia clinical continuum? Aging is the major risk factor for AD[28] and

119   there is increasing evidence that the systems that are vulnerable to AD are also susceptible to the

120   effects of age (see [29–32]). Understanding possible common substrates underlying age-related changes

121   in cortical thickness during development, aging and, dementia can provide valuable understanding

122   of why AD initially targets specific brain networks.

123   **Results**

124

125   Briefly, the MRI and gene expression datasets were parsed into 34 cortical regions-of-interest (ROIs)

126   of the left hemisphere[33]. MRI data were drawn from the Center for Lifespan Changes in Brain and

127   Cognition (LCBC) consisting of 4,004 observations from 1,899 cognitively healthy participants (**Table**

128   **S1**). MRI data were processed through the FreeSurfer pipeline and fitted using generalized additive

129   mixed models (GAMM). Cortical thinning was estimated as the first derivative of the fitted model,

130   and units represent mm of thickness change per year (mm/yr). For gene expression, we used the

131   AHBA, a public resource that includes values of gene expression in multiple regions of the human

132   cerebral cortex. As cell-specific markers, we used genes identified as unique to one of nine cell-types

133   based on single-cell RNA data extracted from the CA1 region and the somatosensory region (S1) in

134   mice[34]. Notably, genes with inconsistent inter-regional profiles of their expression (across donors)

135   and with age-varying profiles were filtered out[24]. As most cortical regions show thinning during the

136   whole lifespan, hereafter we refer to the cortical thinning/thickening estimates by cortical thinning

137   and use the terms "more and less thinning" to denote directionality. Note though that the cortical

138   estimates are measured throughout the thickening/thinning continuum and positive values in the

139   derivative reflect thickening while negative values denote thinning.

140

141   In addition to the main results, we created an interactive resource using the "shiny" R package to

142   allow an interactive visualization of both the trajectories of cortical thickness and thinning

143   throughout the lifespan, and the inter-regional profiles of cortical thinning at any age (**supporting**

144   **information**).

145

146   Lifespan trajectories of cortical thickness and cortical thinning.

147

148   For most regions, the lifespan trajectories of cortical thickness displayed the prototypic pattern

149   characterized by a steep decline in MRI-based estimates of thickness during childhood and

150   adolescence, a mild monotonic thinning from the early adulthood onwards, and a trend towards

151   accelerated thinning in older adulthood (see **Figure 1)**. See an interactive visualization of cortical

152   thickness and thinning trajectories for each region in **supporting information.**
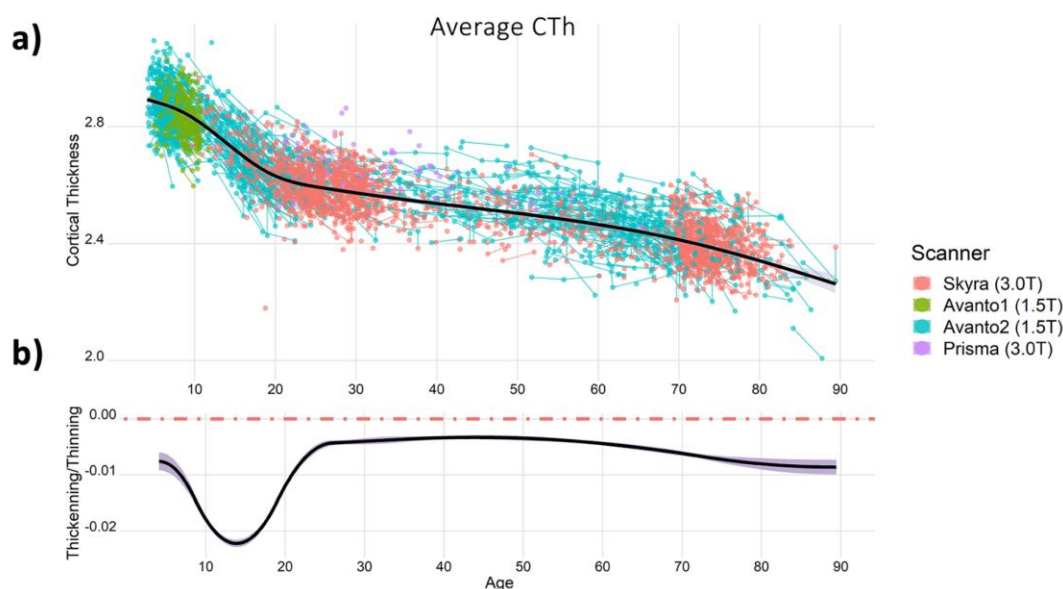

153

154   *Figure 1. Trajectories of weighted-average cortical thickness. The upper and lower plots exhibit the*

155   *trajectories of cortical thickness and cortical thinning during the lifespan, respectively. Cortical*

156   *thickness fitting (black line) overlies a spaghetti plot that displays each observation (dots),*

157   *participant (thin lines) and, scanner (color). The y-axis units represent mm and Δmm/year for the*

158   *thickness and thinning plots, respectively. The dotted red line in the cortical thinning graph*

159   *represents 0 change, negative and positive values represent thinning and thickening, respectively.*

160

161   Lifespan Virtual Histology. Cell type – cortical thinning relationship throughout the lifespan.

162

8

163   Next, we used the virtual histology approach to assess the relationship between cortical thinning

164   across the lifespan and cell-specific gene expression across the 34 cortical regions. In this analysis,

165   we used solely genes with consistent interregional profiles across individual donors and donor age

166   groups. As shown in **Figure 2a,** we observed that the average correlation coefficient for the different

167   cell-types varied throughout the lifespan. The average correlation coefficients differed from the

168   empirical null distributions for the following cell-types and age periods: astrocytes (5 - 11 years, 35 –

169   41 years, 61 - 67 years), microglia (5 - 13 years, 65 - 71 years) and CA1 pyramidal cells (5 - 9 years, 63

170   - 79 years). All results were corrected for both the within (Bonferroni) and between (False Discovery

171   Rate, FDR) cell-type multiple comparisons. Note that the first derivative denotes the degree of

172   thinning so a positive correlation implies that the higher the cell-specific gene expression values are,

173   the less steep the cortical thinning is, and *vice versa*. The average correlation coefficients in

174   childhood/adolescence (for astrocytes, microglia and, CA1 pyramidal cells), and during middle-age

175   (for astrocytes) were positive: thus, cortical regions with higher cell-specific expression for

176   astrocytes, microglia, and CA1 pyramidal cells displayed *less* pronounced thinning. During older age,

177   the gene expression – thinning correlations were negative: thus, cortical regions with higher cell-

178   specific expression for astrocytes, microglia and, CA1 pyramidal cells displayed *more* pronounced

179   age-related cortical thinning. The results were robust to variations of different fitting parameters

180   (**Figure S1, SI Methods, and Results**). The complete statistics are available in **supporting**

181   **information.** Next, we replicated the main findings in three independent datasets that corresponded

182   to the age periods with significant results (i.e. childhood/adolescence, middle-age and older age

183   periods). As seen in **Figure 2b**, we replicated all expression – thinning correlations observed in the

184   discovery sample: positive correlations for astrocytes, microglia and CA1 pyramidal cells in childhood

185   and adolescence, positive correlation for astrocytes in middle-age, and negative correlations for

186   astrocytes, microglia and CA1 pyramidal cells in older age. Note that significance was only tested for

187   the cell types that were significant in the main (discovery) results. See **SI Methods and Results** for a

188   detailed description of the replication results and the samples used.
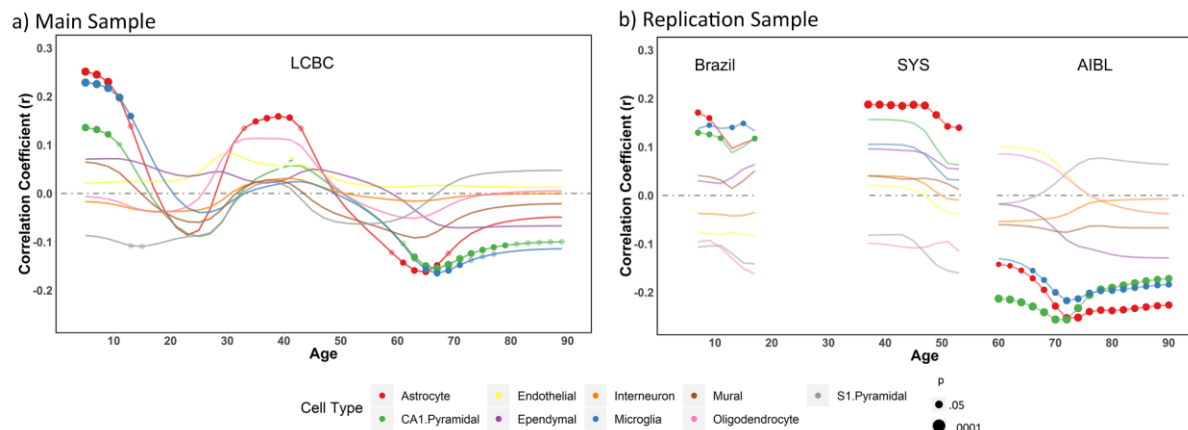
189

190

Figure 2. Virtual Histology through the lifespan. Correlation coefficients between the cortical thinning profile through the lifespan and mean regional profiles of gene expression levels in each of the 9 cell types. a) Thinning profile obtained from the LCBC dataset. (n = 4,004 observations). b) Thinning profile for the replication datasets. SYS replication dataset visualization is trimmed after 55 years to avoid overlap with the AIBL sample (see **SI Methods** for more information). Three different sample cohorts were used corresponding to the age-ranges where significant associations between the thinning profile and cell-specific gene expression were found. We used the Brazil High-Risk Cohort to encompass school years, the SYS dataset for middle-aged participants, and the AIBL data for older adults (n = 1,174, 548 and, 739 observations, respectively). Significance was tested only for significant thinning – expression correlations in the main sample; thus expression – thinning trajectories of the additional cell-types are included for visual purposes only. For both plots, the x-axis indicates age while the y-axis indicates the correlation of thinning with cell type-specific gene expression as derived from the Allen Human Brain Atlas. Values above 0 represent a relationship of gene expression profiles with reduced thinning - or thickening - while values below 0 represent a relationship with steeper cortical thinning. Circles indicate a significant relationship (p < 0.05, permutation inference n = 10,000 iterations) after Bonferroni correction for multiple comparisons through the lifespan (semi-transparent circles) and after additionally applying FDR-adjustment for testing multiple cell-types (opaque circles). The size of the circle represents significance. See the cortical thinning profiles and the expression – thinning correlation results in **Figure 3** and **Table S2**. Post-hoc we tested whether this relationship was evident only for specific subclasses of astrocytes, microglia and CA1 Pyramidal cells. In CA1 pyramidal cells, only expression for the *CA1Pyr2* subclass was associated with young and old cortical thinning profiles (**SI Methods and Results; Table S3**).
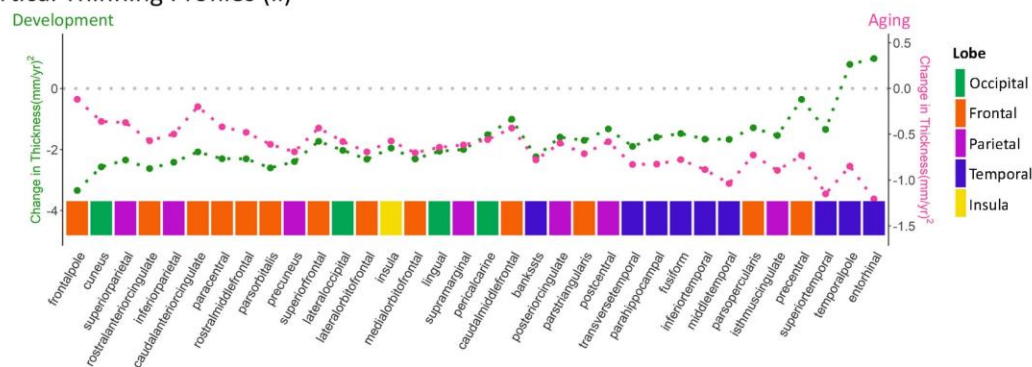
213
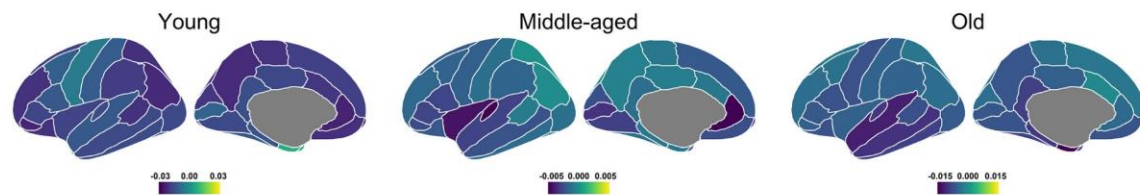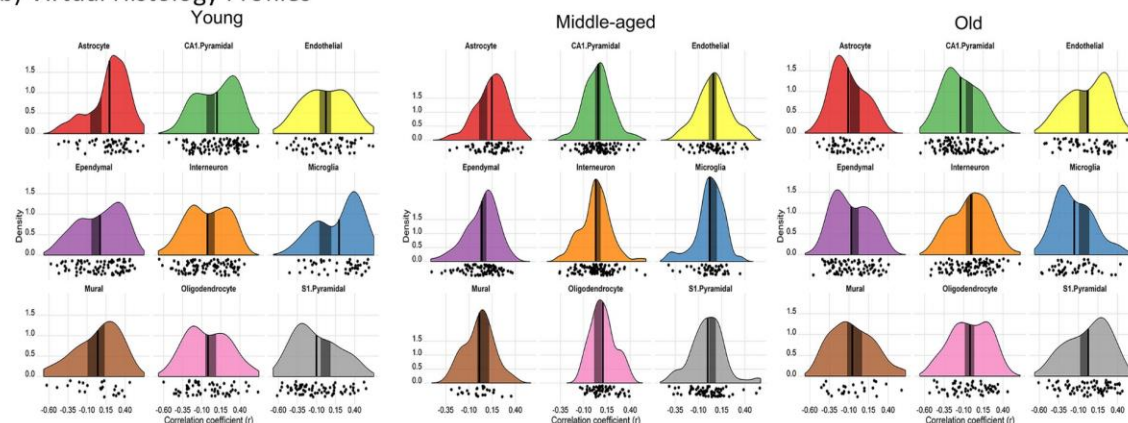
Figure 3. Inter-regional profiles of cortical thinning and Virtual Histology at the ages of interest. *a) Inter-regional patterns of cortical thinning for the age-ranges of interest (i.e. age-periods with significant cell-specific expression-thinning associations), as observed in the LCBC dataset. b) Virtual Histology results (expression – thinning association) for the age-ranges of interest, as observed in the LCBC dataset. Each plot shows the distribution of the expression - thinning correlation coefficients for genes in each cell-type group as a density function and as a cloud of dots. The x-axes indicate the coefficients of correlation between the thinning and the expression profiles. The y-axes indicate the estimated probability density for the correlation coefficients; the vertical black line indicates the average correlation coefficient across all genes while the shaded gray box indicates the 95% limits of the empirical null distribution (unadjusted). From left to right: childhood (5 – 9 years), middle-age (35 -41 years), and old age (63-67 years). See also **Table S2**. c) Inter-regional patterns of cortical thinning*

11

226   *during childhood (5 − 9 years) and at older age (63-67 years). The y-axes denote cortical thinning*

227   *while the x-axis represents each cortical region of the left hemisphere. Regions are also categorized*

228   *by lobe. Note the inverse inter-regional profile of cortical thinning at both ends of the lifespan.*

229

230   Virtual Histology. Cell type – cortical thinning relationship in AD.

231   Next, we tested the relationship between cell-specific gene expression and the patterns of cortical

232   thickness decline related to AD and Mild Cognitive Impairment (MCI). We used the ADNI and AIBL as

233   discovery and replication datasets. We fitted cortical thickness using general linear mixed models

234   (*lme4* R-package), with age, sex and, clinical diagnostic (AD, MCI and cognitively healthy controls

235   [HC]) as fixed effects and participant identifier as a random intercept. The results showed that the

236   different patterns of cortical thinning associated with MCI and AD (AD vs. HC, AD vs. MCI and MCI vs.

237   HC) were all significantly associated with the interregional patterns of gene expression for CA1

238   pyramidal cells, microglia and, astrocytes (see **Figure 4**). Regions with more expression of these

239   markers showed more pronounced thinning. These results were replicated in the AIBL sample. See

240   **Table S4** for complete stats.
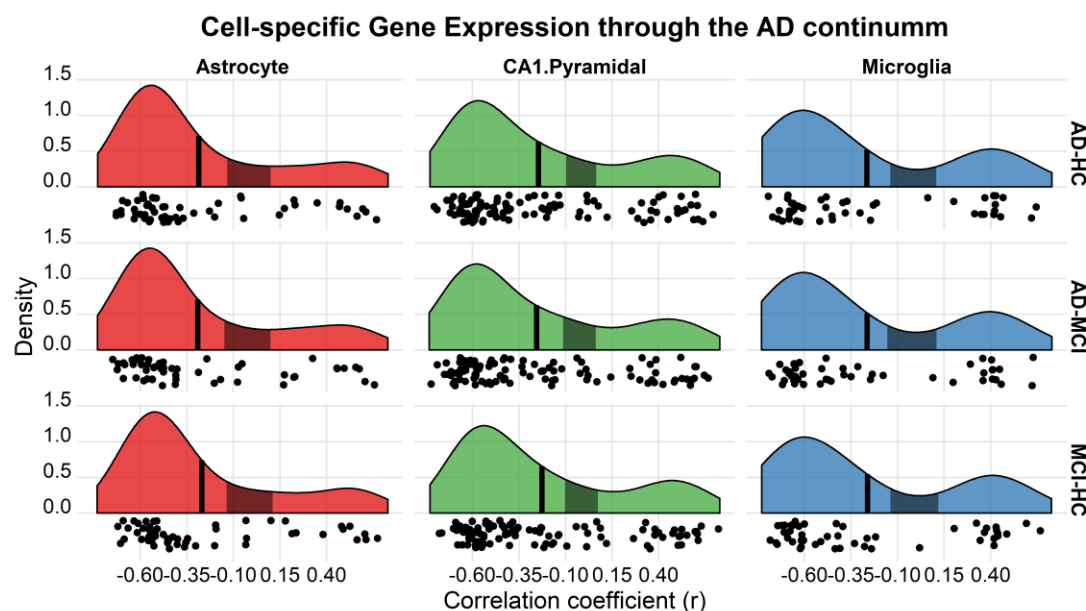

241

242   ***Figure 4. Virtual Histology in AD patterns of cortical thinning.*** *Relationship between cell-specific*

243   *gene expression profiles and the cortical decline in AD (AD vs. HC; AD vs. MCI; MCI vs. AD). Only*

244   *results for the CA1 pyramidal, microglia and, astrocyte cell types are displayed. See **Table S4** for*

245   *complete stats. Each plot shows the distribution of the expression – thinning correlation coefficients*

246   *for genes in each cell-type group. x-axes = coefficients of correlation between the thinning and the*

247   *expression profiles. y-axes = estimated probability density for the correlation coefficients. Vertical*

248   *black line denotes the average correlation coefficient across all genes while the shaded gray box*

249   *indicates the 95% limits of the empirical null distribution.*

250

251   A cortical thickness variation mode as a common mechanism at young and old age as well as in AD.

252

253   Finally, we tested whether the gene expression – cortical thinning relationships at both young and

254   older age are driven by common or different neurobiological mechanisms. For this, we decomposed

255   inter-individual variability in cortical thickness using an Independent Component Analysis (ICA)

256   approach[35,36]. This ICA decomposition approach results in a set of different modes of variation in

257   cortical thickness that can be attributed to plausible, unique, underlying biological mechanisms.

258   Evidence in favor of common mechanisms for the gene – thinning correlations in young and older

259   age should meet the following conditions: i) Evidence of a cortical thickness independent component

260   (IC) with a strong relationship with age. ii) This IC must follow an inverted U-shape lifespan trajectory

261   as the gene expression – cortical thinning relationship at young and old age have opposite directions

262   and; iii) have to relate to the gene expression profiles for CA1 pyramidal, astrocytes, and microglia

263   cell types.

264

265   The results showed three IC components with a relationship with age as assessed with GAMM (r^2 >

266   .15). See **SI Methods** for details. IC1 represented a dominant whole-brain mode of variation; i.e.

267   showing a topological pattern comparable to the mean cortical thickness (r = .45) and a similar

268   lifespan trajectory as the one exhibited by mean cortical thickness, with the steepest decline in late

269   adolescence (highest rate of decline ≈ 18 years of age). A post-hoc analysis (**SI Methods**) suggested

270   that the IC1 cortical loadings are topologically associated with age-related changes in the T1w/T2w

271   index - a putative index of myelination - during this adolescent period (r = .42, p = .014, n = 34 ROIs

272   based on Desikan-Killiany atlas) (**Fig 5a**). This result suggests that some changes in cortical thinning –

273   especially in late adolescence – may be best represented by mean cortical thinning and thus cannot

274   be well-captured by interregional differences in cortical thinning. IC2 component largely captured

275   differences of cortical thickness across scanners as the age effects largely overlap with the density

276   distribution of the different scanners (**Fig 5b**). The utility of the ICA approach for denoising has been

277   discussed elsewhere[37]. Finally, the IC3 component satisfied the predefined conditions. It was

278   strongly related to age (r^2 = .44) and showed an inverted U-shape lifespan trajectory with a steep

279   increase during childhood and a strong decline in old adulthood. Also, the cortical loadings of IC3

280   were related to the interregional patterns of gene expression for CA1 pyramidal, astrocytes and

281   microglia cell-types (all p_{fdr} < .01; the remaining cell type panels were not associated with IC3 p_{fdr} >

282   .05). We ran a post-hoc analysis to test whether genes that co-expressed with cell-specific genes

283   with high fidelity to IC3 were enriched for AD-related genes. The protocol is thoroughly described by

284   Sliz and colleagues[38] and in **SI Methods.** The results of the co-expression, enrichment analysis

285   showed that the set of genes that co-expressed with high IC3 fidelity, microglia-specific, genes were

286   significantly enriched by genes associated with AD (p_{fdr} = .01; **Fig 5c**). CA1 pyramidal (p_{fdr} = .09) and

287   astrocytes (p_{FDR} = .24) co-expressed genes were not enriched for AD genes. Altogether, the results

288   suggest the existence of 1) common mechanisms behind the relationship between cortical thinning

289   and specific cell types at both young and old age that 2) are also disproportionately co-expressed

290   with AD-related genes (only for microglia-specific genes). 3) The presence of different modes of

291   cortical thickness variation during the lifespan that can integrate disparate findings in the literature;

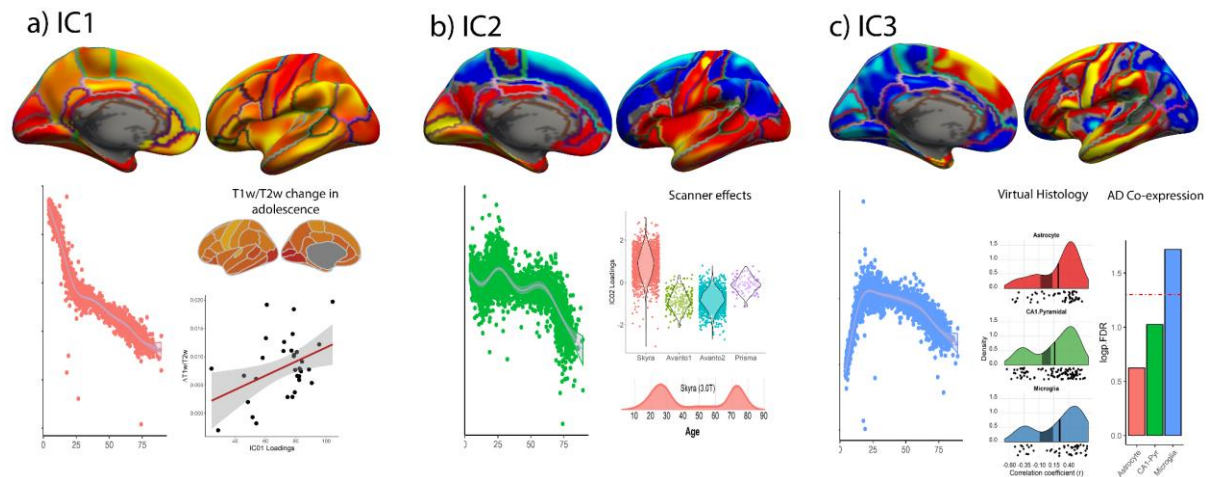292   e.g. myelination vs. dendritic arborization.

Figure 5. Independent components of cortical thickness. *Cortical thickness ICs with practical significance with age (r^2 = .15; arbitrarily thresholded at Z = 4 for visualization). a) Loadings of IC1 through the lifespan. Increase (red-yellow scale) in T1w/T2w ratio during adolescence (mean derivatives between age 15 and age 21). Relationship between T1w/T2w increase during adolescence and IC1 loadings. b) Loadings of IC2 across the lifespan. Loadings of IC2 grouped by scanner. Density function of the Skyra scanner across the lifespan. c) Loadings of IC3 across the lifespan. Relationship between interregional weights of IC3 and cell-specific gene expression for microglia, CA1 pyramidal and, astrocytes. Relationship between AD genes and high-fidelity IC3 cell-specific genes.*

302   **Discussion**

303

304   In this study, we showed that inter-regional profiles of cortical thinning estimated from MRI relate to

305   expression profiles for marker genes of CA1 pyramidal cells, astrocytes and microglia. The

306   relationships were particularly evident during development and aging - higher expression of cell-

307   specific genes was associated with less thinning at younger age (< 13 years of age) and steeper

308   thinning in older age (59 years of age). Similarly, gene expression for CA1 pyramidal cells, astrocytes

309   and microglia were also related to the patterns of cortical thinning both in MCI and AD indicating a

310   continuity throughout development, aging, and disease. The implications of the results are discussed

311   below.

312

313   We found that cell type expression - thinning patterns during development are mirrored later in life.

314   This overarching pattern fits with the view that thinning during developmental and old age periods

315   closely resemble a topography based on common genetic influences[8]. As cortical thinning and thus

316   the expression - thinning correlations change over the lifespan, the associations can be understood

317   at least from three different angles: 1) cortical thinning reflects a direct loss of cell numbers or –

318   more likely – cell volume; 2) cell-specific processes – e.g. apoptosis or metabolic demands –mediate

319   indirectly the relationship between cell-type and thinning of the cerebral cortex; and 3) an

320   interaction between developmental (or neurodegenerative) processes and MRI acquisition

321   parameters or analytical features – e.g. shifts in T1/T2 boundary delineation may occur due to

322   myelination[11].

323

324   The association of astrocytes, microglia and CA1 pyramidal cells with less cortical thinning during

325   development replicate our earlier findings in an independent, cross-sectional adolescent sample[24].

16

326   The involvement of CA1 pyramidal cells with less cortical thinning is in agreement with the notion

327   that axonal sprouting and remodeling of dendritic arbor are associated with relative thickening of

328   the developing cerebral cortex[24]. CA1 pyramidal genes are highly enriched for terms such as

329   "regulation of dendrite extension" in contrast with S1 pyramidal genes, enriched by terms associated

330   with potassium transport and activity[24]. A plausible theory is that the thinning profiles in childhood

331   and early adolescence are partly dependent on the regional dynamics and regional differences in

332   dendritic growth[39,40]. Note that these findings are not in opposition – but rather complementary -

333   with evidence that myelin is an important process behind cortical thinning during development[23,25].

334   See *considerations* for an extended discussion.

335

336   In aging, regions with high CA1 pyramidal expression coincide with those undergoing steeper

337   thinning. This observation fits with both existing histological evidence and current predictions that

338   link dendritic shrinkage with reduced cortical thickness in older brains[16–18,41]. Although neuronal

339   numbers seem preserved in aging[20,41], recent evidence suggests that specific neural subpopulations

340   numbers – namely neurons with large cell bodies (and possibly larger dendritic arbour) – might

341   decrease in aged brains[42]. Again, S1 pyramidal expression was unrelated to thinning with advancing

342   age, which is consistent with evidence that neuron-specific changes of gene expression with age are

343   dependent on cellular identity[42,43]. A promising direction requires linking variations of neuronal

344   properties[45] – including regional variations in dendritic and soma size - with MRI estimates of cortical

345   thinning. As a proof of principle, we found that for CA1 pyramidal cells, only expression for the

346   *CA1Pyr2* subclass was associated with the thinning profiles (**SI Methods and Results**). Expression of

347   *CA1Pyr2*-specific genes is associated with mitochondrial function, which correlates with the length of

348   projections in cortical neurons[34].

349

350   Expression of genes specific to astrocytes and microglia was associated with cortical thinning in both

351   younger and older ages. Despite modest changes in the cell numbers[20,45] and cell morphology

352   throughout the lifespan[46,47], it is more likely that the relationship between cortical thinning and

353   these glial subpopulations relates to interactions with other neural components such as astrocytic

354   metabolic processes and signaling pathways for microglia. Astrocytes distribute energy substrates –

355   mostly lactate – to active neurons[48,49], sustaining glutamatergic neurotransmission, synaptic

356   plasticity, and thus long-term memory formation[50]. Microglia engage in crosstalk with neurons and

357   astrocytes, can modulate synaptic homeostasis, remodel synaptic structures (e.g., dendritic spines),

358   and is closely involved in the maintenance of neuronal structure and function. Likewise, both cell-

359   types are up-regulated homogenously in the cerebral cortex with advancing age[42,43], leaning towards

360   a reactive phenotype for astrocytes and a shift to a pro-inflammatory profile for microglia[51,52].

361   Altogether, we speculate that in childhood and adolescence, astrocytic and microglia relate to

362   regional preservation of cortical thickness by promoting and supporting neuronal development, such

363   as dendritic arborization and synaptic remodeling. In aging, failure or dysregulation of upstream

364   microglia and astrocyte cellular processes might lead to dendritic and synaptic changes and

365   subsequent loss of cortical thickness.

366

367   Expression – thinning associations during the lifespan were reproduced in AD. That is, gene

368   expression for microglia, astrocytes and, CA1 pyramidal cells related to the characteristic pattern of

369   cortical thinning in AD. Synapse loss is a key feature of AD[53,54] while astrocytes and microglia play

370   various roles in the AD cellular and molecular cascade[30]. Astrocytes produce ApoliproteinE[55] and

371   have a possible role in glucose hypometabolism[56] and together with microglia they adopt a reactive

372   profile and play a fundamental role in the inflammatory changes in the brain[51,52]. While the results

373   likely reflect several molecular mechanisms, they hint to a last-in, first-out lifespan system with

374   heightened vulnerability to AD. One may speculate, the system is characterized by neural bodies

18

375   with higher energetic demands, more complex synaptic and dendritic patterns and higher plasticity.

376   In any case, the continuous relationship between cell-specific gene expression and cortical thinning

377   through development, aging and disease points both towards the notion of system's vulnerability

378   and that – to some extent - differences in AD (vs. MCI and cognitively healty older adults) can be

379   better clarified by understanding age-related changes in healthy aging.

380

381   *Considerations.* Two features of the study require special consideration, namely the source of

382   variability and the correlational nature of the analyses. Correlational tests are unavoidable when

383   exploring the underlying mechanisms of cortical thinning *in vivo*, yet longitudinal comparisons (i.e.

384   individual rates of thinning) will approximate better the dynamic relationship of thinning and its

385   neurobiological foundations across the lifespan.

386

387   The main measure of the study is the interregional profile of cortical thinning at different ages.

388   While it represents a robust and stable measure, the interregional thinning profile is unable to

389   provide information neither at an individual level nor across time; hence, a portion of the variability

390   remains unexplored. The relative disparity amongst studies might reside on different

391   characterizations of cortical thinning variability, especially during development. In particular, MRI

392   estimates of myelin content have repeatedly been associated with steeper cortical thinning in

393   adolescents[23,25]. Here, lack of findings may relate to the nature of the interregional profiles, which

394   represent snapshots in time and, hence, are determined by the differential sum of processes that

395   modulate cortical thickness in each area. In other words, interregional comparisons cannot evaluate

396   mean (whole-brain) cortical thinning. Further, the cellular correlates of cortical thinning during

397   childhood in the present study relate to *spared* thinning, which points out that these mechanisms

398   are supplementary to those that drive cortical thinning during adolescence. The ICA analysis

399   tentatively integrates both findings. On one side, we found a main component of cortical thickness

400 variability that displayed topological and lifespan trajectories – such as a steep decline in

401 adolescence - that evoke those of mean cortical thickness. This component related to T1w/T2w

402 signal increase during adolescence, a putative index of myelination[57]. One can speculate that this

403 pattern is concealed in the interregional approach due to its similarity to mean cortical thinning[25].

404 On the other side, a second component linked both the expression – thinning relationships during

405 development and aging and further extend it to AD. As interregional variability in cortical thinning is

406 quite substantial – with some regions showing significant thickening during childhood – the results

407 pinpoint to the presence of complementary processes in development that require further

408 understanding. Altogether, the results suggest that, at least in early phases of life, diverging

409 mechanisms promote at the same time thinning and thickening of the cerebral cortex[41].

410

411 **Conclusion**

412

413 Understanding the biological substrate underlying MRI-based estimates of cortical thinning during

414 different stages of the lifespan remains a key issue in neuroscience given the ever-increasing use of

415 neuroimaging and the association of variations in cortical thickness with neurodevelopmental and

416 neurodegenerative pathology. We found that cortical thinning was associated with the expression of

417 genes specific to CA1 pyramidal cells, astrocytes, and microglia in both development and in aging.

418 This expression – thinning relationship was conserved in AD. The study informs of a common

419 biological substrate that affects cortical thickness and links development, aging and systems

420 vulnerability to AD. We speculate that microglia and astrocytic functions are essential for promoting

421 and supporting neuronal growth and development in childhood and thus relative regional

422 preservation of thickness in childhood. Failure of these upstream processes might lead to dendritic

423 changes and subsequent cortical thinning in aging.

20

Material and methods

MRI sample

A total of 4,004 scans from 1,899 healthy participants (1,135 females) ranged between 4.1 – 89.4 years of age (mean visit age = 37.4 [SD = 25.3]) (**Figure 1; Table S1**) were drawn from six Norwegian studies coordinated by the Center for LCBC: The Norwegian Mother and Child Cohort Neurocognitive Study[58]; Neurocognitive Development[59]; Cognition and Plasticity Through the Lifespan[60]; Constructive Memory[61]; Method of Loci[62]; and Neurocognitive plasticity[63]. More than one scan was available for 1,017 participants; the mean number of scans per participant was 2.1 (range 1-6) spanning up to 11.1 years after the initial scan. The density of sampling was higher in childhood/adolescence and during the 7th and 8th decade of life. See **Figure S2** and **Table S1** for visual representation and descriptive information.

In all studies, participants were screened through health and neuropsychological assessments. Common exclusion criteria consisted of evidence of neurologic or psychiatric disorders, learning disabilities or current use of medicines known to affect the nervous system. In addition, participants were excluded from the current study based on the following criteria: lack of a valid structural scan (i.e. excessive movement, acquisition or surface reconstruction errors), score <25 on the Mini-Mental State Examination (MMSE)[63], score of ≥20 on the Beck Depression Inventory (BDI)[65], and age > 90 due to low sampling density after this age. All the studies were approved by a Norwegian Regional Committee for Medical and Health Research Ethics. See **SI Methods** for further details on samples.

448   For replication, we used three additional samples that encompassed the age periods in which we

449   observed associations between regional patterns of cortical thinning and cell-specific gene

450   expression. We used the Brazil High-Risk Cohort[66] to replicate findings during

451   childhood/adolescence. For replication of results in middle-age, we used the cohort of parents of the

452   Saguenay Youth Study (SYS)[67]. For older adults, the replication sample was collected by the AIBL

453   study group. AIBL study methodology has been reported previously[68]. See **Figure S2, Table S5** and, **SI**

454   **Methods** for the replication sample description.

455

456   We used the ADNI database (adni.loni.usc.edu)[69] (discovery) and AIBL[68] (replication) samples to

457   estimate the patterns of cortical thinning in AD. ADNI was launched in 2003 as a public-private

458   partnership, led by PI MW Weiner. The primary goal of ADNI has been to test whether serial MRI,

459   other biological markers, and clinical and neuropsychological assessments can measure the

460   progression of MCI and early AD. The *Australian Imaging, Biomarker & Lifestyle Flagship Study of*

461   *Ageing (AIBL)* took place in Australia, beginning in 2006, with the aim to study which biomarkers,

462   cognitive characteristics, and health and lifestyle factors determine the development of AD. See

463   **Table S6** and **SI Methods** for further description

464

465   MRI acquisition and preprocessing

466

467   LCBC image data were collected using four different scanners. Three scanners (*Avanto2 [1.5 T],*

468   *Prisma [3.0 T] and Skyra [3.0 T];* Siemens Medical Solution) were located at Oslo University Hospital

469   Rikshospitalet while the remaining (*Avanto1 [1.5 T])* was placed at St. Olav's University Hospital in

470   Trondheim. For 285 participants, data were available for two or more MRI machines from the same

471   day (n = 285). For each participant and visit, we obtained a T1w magnetization prepared rapid

472   gradient echo (MPRAGE) sequence. See **SI Methods** for MRI acquisition parameters in both the LCBC

473   and the replication datasets.

474

475   Data were processed on the Colossus processing cluster, University of Oslo. We used the

476   longitudinal FreeSurfer v.6.0. stream[70] for cortical reconstruction of the structural T1w data

477   (http://surfer.nmr.mgh.harvard.edu/fswiki)[71–73]. See the pipeline description in **SI Methods**. See **SI**

478   **Methods** for differences in the MRI processing pipeline in the replication datasets.

479

480   MRI analysis. Estimation of cortical thinning through the lifespan.

481

482   After the surface reconstruction, MRI-based estimates of cortical thickness were extracted for the 34

483   left hemisphere ROIs corresponding to the Desikan-Killiany atlas[33]. We ran an analysis to estimate

484   each region's cortical thinning - or thickening - at any given point during the lifespan. First, for each

485   of the 34 cortical regions, thickness data were fitted to age using GAMM with "mgcv" R package[74].

486   The GAMM fitting technique represents a flexible routine that allows nonparametric fitting with

487   relaxed assumptions about the relationship between thickness and age[8]. The technique is well suited

488   for fitting nonlinear relationships through local smoothing effects, independent of any predefined

489   model, and robust to age-range selections and distant data points[75].

490

491   All GAMM models included sex and scanner as covariates and participant identifiers as random

492   effects. We specified cubic splines as smooth terms[74] and limited to k = 6 the knots of the spline, a

493   somewhat conservative option to minimize the risk of overfitting and to increase the stability of the

494   derivatives. Next, we excluded those observations ± 7 SD above or below the cortical thickness

23

495   trajectory (mean = 3.2 [1.8 SD] observations excluded per region). After outlier removal, cortical

496   thickness data were re-fitted by age with GAMM (separately in each region).

497

498   Finally, we considered the GAMM derivatives to obtain the trajectories of cortical thinning

499   throughout the lifespan. For each region, we obtained the derivative – and its confidence intervals -

500   based on a finite differences approach as implemented in the *"schoenenberg"* R package

501   (https://github.com/gavinsimpson/schoenberg). Positive values in the derivative are interpreted as

502   steeper thickening while negative values are interpreted as steeper thinning at any given age. For

503   each cortical region, we then extracted the derivative values at discrete ages (from 5 to 89 years;

504   every 2 years) resulting in n = 43 cortical thinning profiles spanning from childhood to old adulthood.

505

506   Gene expression analysis. Estimation of cell-specific gene expression across the cortical surface.

507

508   We used the scripts provided by Shin and colleagues[24] to obtain gene expression profiles across the

509   left hemisphere. Note that only genes with inter-regional profiles consistent across the six donors

510   (AHBA) and across two datasets (AHBA and the BrainSpan Atlas) were used. See **SI methods** and

511   elsewhere and elsewhere [24] for details.

512

513   Gene expression profile: Gene expression data were obtained from the AHBA, based on postmortem

514   human brains, providing comprehensive coverage of the normal adult brain (http://www.brain-

515   map.org)[27]. Isolated RNA was hybridized to custom 64K Agilent microarrays (58,692 probes) by the

516   Allen Institute. Gene expression data for the left hemisphere were available for six donors.

517

518   As described previously[76], gene-expression data from the AHBA were mapped to the Desikan-Killiany

519   atlas in FreeSurfer space yielding up to 1,269 labeled samples per brain inside or close to a

24

520   FreeSurfer cortical region[33]. The expression values of the mapped samples were mean averaged

521   across microarray probes to provide a single expression value for each gene for a given sample.

522   Median averages were used to summarize expression values within each ROI and donor, which was

523   followed by the median average across the six donors. This yielded a single value for each region

524   representing the median profile for a given gene across the 34 cortical regions.

525

526   Panels of Cell-Specific Marker Genes: Lists of genes expressed in specific cell types were obtained

527   from Zeisel and colleagues[34]. In their study, single-cell transcriptomes were obtained for 3,005 cells

528   from the somatosensory cortex (S1) and the CA1 hippocampus region of mice. Gene expression was

529   then biclustered into nine classes that contained each over 100 genes. We converted mouse genes

530   to human gene symbols as implemented in the *"homologene"* R package[77]. The resulting classes of

531   cell types and the number of marker genes kept after consistent genes were filtered are: S1

532   pyramidal neurons (n = 73 human gene symbols), CA1 pyramidal neurons (n = 103), interneurons (n

533   = 100), astrocytes (n = 54), microglia (n = 48), oligodendrocytes (n = 60), ependymal (n = 84),

534   endothelial (n = 57), and mural (pericytes and vascular smooth muscle cells; n = 25).

535

536   Higher-level statistical analysis

537

538   All the in-house procedures were implemented in R (www.r-project.org). Figures were created using

539   ggplot, FreeSurfer viewers and the ggseg package[78,79].

540

541   Correlation between lifespan thinning and cell-specific gene expression profiles: In the main analysis,

542   we assessed the relationship between the inter-regional profiles of cortical thinning – obtained from

543   the GAMM derivative sampled between 5 and 89 years - and the inter-regional profiles of gene

544   expression associated with specific cell types. For each cortical profile and marker gene, we

545   computed the Pearson correlation coefficients between the thinning profile and the median inter-

546   regional profile of gene expression levels for each marker gene; yielding a gene-specific measure of

547   expression - thinning correlation.

548

549   We used a resampling-based approach to test the association between cell-type expression and

550   cortical thinning profiles[24]. The average expression - thinning correlation for each group of cell-

551   specific genes served as the test statistic (i.e. mean correlation between cortical phenotype and cell-

552   specific gene expression). In addition, we controlled for multiple comparisons, accounting both for

553   the number of cortical thinning profiles (i.e. age points n = 43) and for the different cell-types (n = 9).

554

555   For each cell-type panel, we obtained the empirical null distribution of the test statistic as follows. 1)

556   From all the (n = 2,511) consistent genes, we randomly selected the same number of genes as that

557   of the genes in the cell-type group under consideration. 2) For each thinning profile (n = 43 sampled

558   ages), we averaged the expression - thinning correlation coefficients of all the selected genes. Thus,

559   for each random sample, we obtained the mean correlation coefficients at each age. 3) Of the n = 43

560   coefficients, we selected the one with absolute maximum expression - thinning correlation. This step

561   is essential to introduce a Bonferroni-like correction for multiple comparisons at a within cell-type

562   level while accounting for the non-independency of the thinning estimates (e.g. the cortical thinning

563   profiles at age 60 and 62 are not independent observations). The null distribution was estimated by

564   repeating the previous three steps for 10,000 iterations. A two-sided p-value was computed as the

565   proportion of average thinning – expression correlations whose values exceeded the average for the

566   genes in the original cell-type group. We rejected the null hypothesis at p = .05 FDR-adjusted

567   significance thus correcting for multiple testing of the nine cell-type groups.

568

569   The same procedure was run for the three replication-samples with the following variations. The

570   number of within cell-type comparisons was defined by the specific age range of each replication

571   sample (n = 6, 15 and 17 2-year steps for Brazil, SYS, and AIBL datasets, respectively). Second,

572   significance testing and FDR between cell-type corrections were only applied for those cell-type

573   groups that were significant in the main analysis.

574

575   We used a similar *Virtual Histology* analysis to assess the relationship between gene expression and

576   cortical thinning in AD. For each ROI (n = 34), we modelled the effect of clinical diagnosis on cortical

577   thickness with linear mixed models as implemented in *lme4*. The models also included magnetic

578   field/site (ADNI/AIBL), age and sex as fixed effects and a subject identifier modelled as random

579   intercepts. Significance testing was applied through permutation testing[24], further corrected for

580   multiple comparisons for the different cell-type panels (n = 9; FDR-corrected).

581

582   Independent Component Analysis

583   We used an ICA as implemented in FLICA[35,36] with 70 components[80] to derive modes of cortical

584   thickness variability. For each IC, we initially tested the relationship with age using GAMM models.

585   Following existing work[80,81], only components with a strong *practical* significance ($r^2 > .15$) were

586   considered for further analysis. See **SI Methods** for more details.

587

588   *Post-hoc analyses with the IC components.* We tested the topological relationship between cortical

589   thickness, T1w/T2w change during adolescence – as an index of myelination – and IC1 cortical

590   weights using Pearson's correlation. For T1w/T2w, we used a subset of LCBC participants (age = 8 –

591   40 years) with an available T2w sequence. We preprocessed the data using Human Connectome

592   Project (HCP) processing pipeline[82] (https://github.com/Washington-University/Pipelines) and

593   summarized the T1w/T2w values – sampled at 70% from the WM/GM boundary[83] - using the

594   Desikan-Killiany parcellation. T1w/T2w values were fitted to age using splines and the mean

595   derivative values between 15 and 21 were selected as the index of interest (age epoch where IC1

596   showed maximal decrements). See Grydeland and colleagues[84] and **SI Methods** for more details. For

597   IC2, scanner effects were tested using GAMM with scanner and sex as fixed effects, age as

598   smoothing term and, participant as random effects. We used *geom_violin* and *geom_density*

599   functions to visualize the relationship between scanner effect and scanner distribution through the

600   lifespan with IC2 loading. For IC3, we performed a *virtual histology* analysis as described above,

601   using IC3 cortical loadings as the phenotype of interest. Further, we used a co-expression analysis to

602   test whether high-fidelity IC3 astrocytes, microglia and, CA1 pyramidal-specific genes were enriched

603   for AD. Briefly, we created a co-expression data matrix based on available gene expression brain

604   banks[26,84–87] and overexpression for AD genes was then tested using an AD geneset curated by the

605   DisGeNET database[89]. See **SI Methods** for more details.

Acknowledgments

631 Foundation for the National Institutes of Health (www.fnih.org). The grantee organization is the

632 Northern California Institute for Research and Education, and the study is coordinated by the

633 Alzheimer's Therapeutic Research Institute at the University of Southern California. ADNI data are

634 disseminated by the Laboratory for Neuro Imaging at the University of Southern California.

635 **Author Contributions**

636

637 D.V.P, T.P., A.M.F, Z.P., and K.B.W. designed the study; A.P.J., G.S., and AIBL collected data; D.V.P,

638 N.P., J.S., L.F., H.G., A.M.M., Y.P., and Ø.S. performed the analyses, created the figures. The paper

639 was written by D.V.P, T.P. and, A.M.F with input from all the authors.

640

641   **Competing Interests statement**

642

643   The authors declare no competing financial interests.

644

645 **Data availability**

646

647 The authors will provide the code upon acceptance at https://github.com/LCBC-
648 UiO/virtual_histology_2019.

649

Data availability

650

References

1. Walhovd, K. B. *et al.* Long-term influence of normal variation in neonatal characteristics on human brain development. *Proc. Natl. Acad. Sci. U.S.A.* **109**, 20089–20094 (2012).

2. Miller, K. L. *et al.* Multimodal population brain imaging in the UK Biobank prospective epidemiological study. *Nat. Neurosci.* **19**, 1523–1536 (2016).

3. Jack, C. R. *et al.* Different definitions of neurodegeneration produce similar amyloid/neurodegeneration biomarker group findings. *Brain* **138**, 3747–3759 (2015).

4. Jack, C. R. *et al.* NIA-AA Research Framework: Toward a biological definition of Alzheimer's disease. *Alzheimers Dement* **14**, 535–562 (2018).

5. Grasby, K. L. *et al.* The genetic architecture of the human cerebral cortex. *Science* **367**, (2020).

6. Shin, J. *et al.* Global and Regional Development of the Human Cerebral Cortex: Molecular Architecture and Occupational Aptitudes. *Cereb. Cortex* (2020) doi:10.1093/cercor/bhaa035.

7. Fjell, A. M. *et al.* Development and aging of cortical thickness correspond to genetic organization patterns. *Proc. Natl. Acad. Sci. U.S.A.* **112**, 15462–15467 (2015).

8. Paus, T. Imaging microstructure in the living human brain: A viewpoint. *Neuroimage* **182**, 3–7 (2018).

9. Fjell, A. M. *et al.* One-year brain atrophy evident in healthy aging. *J. Neurosci.* **29**, 15223–15231 (2009).

10. Walhovd, K. B., Fjell, A. M., Giedd, J., Dale, A. M. & Brown, T. T. Through Thick and Thin: a Need to Reconcile Contradictory Results on Trajectories in Human Cortical Development. *Cereb. Cortex* **27**, 1472–1481 (2017).

11. Huttenlocher, P. R. Synaptic density in human frontal cortex - developmental changes and effects of aging. *Brain Res.* **163**, 195–205 (1979).

675   12. Huttenlocher, P. R. & Dabholkar, A. S. Regional differences in synaptogenesis in human cerebral

676   cortex. *J. Comp. Neurol.* **387**, 167–178 (1997).

677   13. Sowell, E. R. *et al.* Longitudinal mapping of cortical thickness and brain growth in normal

678   children. *J. Neurosci.* **24**, 8223–8231 (2004).

679   14. Paus, T., Keshavan, M. & Giedd, J. N. Why do many psychiatric disorders emerge during

680   adolescence? *Nat. Rev. Neurosci.* **9**, 947–957 (2008).

681   15. Peters, A. & Sethares, C. The effects of age on the cells in layer 1 of primate cerebral cortex.

682   *Cereb. Cortex* **12**, 27–36 (2002).

683   16. Lu, T. *et al.* Gene regulation and DNA damage in the ageing human brain. *Nature* **429**, 883–891

684   (2004).

685   17. Esiri, M. M. Ageing and the brain. *J. Pathol.* **211**, 181–187 (2007).

686   18. Dickerson, B. C. *et al.* The cortical signature of Alzheimer's disease: regionally specific cortical

687   thinning relates to symptom severity in very mild to mild AD dementia and is detectable in

688   asymptomatic amyloid-positive individuals. *Cereb. Cortex* **19**, 497–510 (2009).

689   19. Sloper, J. J., Hiorns, R. W. & Powell, T. P. A qualitative and quantitative electron microscopic

690   study of the neurons in the primate motor and somatic sensory cortices. *Philos. Trans. R. Soc.*

691   *Lond., B, Biol. Sci.* **285**, 141–171 (1979).

692   20. Pelvig, D. P., Pakkenberg, H., Stark, A. K. & Pakkenberg, B. Neocortical glial cell numbers in

693   human brains. *Neurobiol. Aging* **29**, 1754–1762 (2008).

694   21. Druga, R. Neocortical inhibitory system. *Folia Biol. (Praha)* **55**, 201–217 (2009).

695   22. Carlo, C. N. & Stevens, C. F. Structural uniformity of neocortex, revisited. *Proc. Natl. Acad. Sci.*

696   *U.S.A.* **110**, 1488–1493 (2013).

697   23. Natu, V. S. *et al.* Apparent thinning of human visual cortex during childhood is associated with

698   myelination. *Proc. Natl. Acad. Sci. U.S.A.* **116**, 20750–20759 (2019).

699   24. Shin, J. *et al.* Cell-Specific Gene-Expression Profiles and Cortical Thickness in the Human Brain.

700   *Cereb. Cortex* **28**, 3267–3277 (2018).

36

701   25. Whitaker, K. J. *et al.* Adolescence is associated with genomically patterned consolidation of the

702   hubs of the human brain connectome. *Proc. Natl. Acad. Sci. U.S.A.* **113**, 9105–9110 (2016).

703   26. Hawrylycz, M. J. *et al.* An anatomically comprehensive atlas of the adult human brain

704   transcriptome. *Nature* **489**, 391–399 (2012).

705   27. Kawas, C., Gray, S., Brookmeyer, R., Fozard, J. & Zonderman, A. Age-specific incidence rates of

706   Alzheimer's disease: the Baltimore Longitudinal Study of Aging. *Neurology* **54**, 2072–2077

707   (2000).

708   28. Herrup, K. Reimagining Alzheimer's disease--an age-based hypothesis. *J. Neurosci.* **30**, 16755–

709   16762 (2010).

710   29. Tse, K.-H. & Herrup, K. Re-imagining Alzheimer's disease - the diminishing importance of amyloid

711   and a glimpse of what lies ahead. *J. Neurochem.* **143**, 432–444 (2017).

712   30. Jagust, W. Vulnerable neural systems and the borderland of brain aging and neurodegeneration.

713   *Neuron* **77**, 219–234 (2013).

714   31. Fjell, A. M. *et al.* What is normal in normal aging? Effects of aging, amyloid and Alzheimer's

715   disease on the cerebral cortex and the hippocampus. *Prog. Neurobiol.* (2014)

716   doi:10.1016/j.pneurobio.2014.02.004.

717   32. Desikan, R. S. *et al.* An automated labeling system for subdividing the human cerebral cortex on

718   MRI scans into gyral based regions of interest. *Neuroimage* **31**, 968–980 (2006).

719   33. Zeisel, A. *et al.* Brain structure. Cell types in the mouse cortex and hippocampus revealed by

720   single-cell RNA-seq. *Science* **347**, 1138–1142 (2015).

721   34. Groves, A. R. *et al.* Benefits of multi-modal fusion analysis on a large-scale dataset: life-span

722   patterns of inter-subject variability in cortical morphometry and white matter microstructure.

723   *Neuroimage* **63**, 365–380 (2012).

724   35. Groves, A. R., Beckmann, C. F., Smith, S. M. & Woolrich, M. W. Linked independent component

725   analysis for multimodal data fusion. *Neuroimage* **54**, 2198–2217 (2011).

726   36. Li, H. *et al.* Denoising scanner effects from multimodal MRI data using linked independent

727   component analysis. *Neuroimage* **208**, 116388 (2020).

728   37. Sliz, E. *et al.* A variant near DHCR24 associates with microstructural properties of white matter

729   and peripheral lipid metabolism in adolescents. *Mol Psychiatry* 1–11 (2020) doi:10.1038/s41380-

730   019-0640-9.

731   38. Petanjek, Z. *et al.* Extraordinary neoteny of synaptic spines in the human prefrontal cortex. *Proc.*

732   *Natl. Acad. Sci. U.S.A.* **108**, 13281–13286 (2011).

733   39. Elston, G. N. & Fujita, I. Pyramidal cell development: postnatal spinogenesis, dendritic growth,

734   axon growth, and electrophysiology. *Front Neuroanat* **8**, 78 (2014).

735   40. Fjell, A. M. & Walhovd, K. B. Structural brain changes in aging: courses, causes and cognitive

736   consequences. *Rev Neurosci* **21**, 187–221 (2010).

737   41. Pakkenberg, B. *et al.* Aging and the human neocortex. *Exp. Gerontol.* **38**, 95–99 (2003).

738   42. Soreq, L. *et al.* Major Shifts in Glial Regional Identity Are a Transcriptional Hallmark of Human

739   Brain Aging. *Cell Rep* **18**, 557–570 (2017).

740   43. French, L., Ma, T., Oh, H., Tseng, G. C. & Sibille, E. Age-Related Gene Expression in the Frontal

741   Cortex Suggests Synaptic Function Changes in Specific Inhibitory Neuron Subtypes. *Front Aging*

742   *Neurosci* **9**, 162 (2017).

743   44. Scholtens, L. H., Schmidt, R., de Reus, M. A. & van den Heuvel, M. P. Linking macroscale graph

744   analytical organization to microscale neuroarchitectonics in the macaque connectome. *J.*

745   *Neurosci.* **34**, 12192–12205 (2014).

746   45. VanGuilder, H. D. *et al.* Concurrent hippocampal induction of MHC II pathway components and

747   glial activation with advanced aging is not correlated with cognitive impairment. *J*

748   *Neuroinflammation* **8**, 138 (2011).

749   46. Jyothi, H. J. *et al.* Aging causes morphological alterations in astrocytes and microglia in human

750   substantia nigra pars compacta. *Neurobiol. Aging* **36**, 3321–3333 (2015).

751   47. Pellerin, L. & Magistretti, P. J. Glutamate uptake into astrocytes stimulates aerobic glycolysis: a

752   mechanism coupling neuronal activity to glucose utilization. *Proc. Natl. Acad. Sci. U.S.A.* **91**,

753   10625–10629 (1994).

754   48. Pellerin, L. & Magistretti, P. J. Sweet sixteen for ANLS. *J. Cereb. Blood Flow Metab.* **32**, 1152–

755   1166 (2012).

756   49. Alberini, C. M., Cruz, E., Descalzi, G., Bessières, B. & Gao, V. Astrocyte glycogen and lactate: New

757   insights into learning and memory mechanisms. *Glia* **66**, 1244–1262 (2018).

758   50. Olah, M. *et al.* A transcriptomic atlas of aged human microglia. *Nat Commun* **9**, 539 (2018).

759   51. Clarke, L. E. *et al.* Normal aging induces A1-like astrocyte reactivity. *Proc. Natl. Acad. Sci. U.S.A.*

760   **115**, E1896–E1905 (2018).

761   52. DeKosky, S. T. & Scheff, S. W. Synapse loss in frontal cortex biopsies in Alzheimer's disease:

762   correlation with cognitive severity. *Ann. Neurol.* **27**, 457–464 (1990).

763   53. Terry, R. D. *et al.* Physical basis of cognitive alterations in Alzheimer's disease: synapse loss is the

764   major correlate of cognitive impairment. *Ann. Neurol.* **30**, 572–580 (1991).

765   54. Fagan, A. M. *et al.* Unique lipoproteins secreted by primary astrocytes from wild type, apoE (-/-),

766   and human apoE transgenic mice. *J. Biol. Chem.* **274**, 30001–30007 (1999).

767   55. Carter, S. F. *et al.* Astrocyte Biomarkers in Alzheimer's Disease. *Trends Mol Med* **25**, 77–95

768   (2019).

769   56. Glasser, M. F. & Van Essen, D. C. Mapping human cortical areas in vivo based on myelin content

770   as revealed by T1- and T2-weighted MRI. *J. Neurosci.* **31**, 11597–11616 (2011).

771   57. Krogsrud, S. K. *et al.* Development of hippocampal subfield volumes from 4 to 22 years. *Hum

772   Brain Mapp* **35**, 5646–5657 (2014).

773   58. Tamnes, C. K. *et al.* Intellectual abilities and white matter microstructure in development: a

774   diffusion tensor imaging study. *Hum Brain Mapp* **31**, 1609–1625 (2010).

775   59. Fjell, A. M. *et al.* The relationship between diffusion tensor imaging and volumetry as measures

776   of white matter properties. *Neuroimage* **42**, 1654–1668 (2008).

777   60. Sneve, M. H. *et al.* Mechanisms underlying encoding of short-lived versus durable episodic

778   memories. *J. Neurosci.* **35**, 5202–5212 (2015).

779   61. Engvig, A. *et al.* Effects of memory training on cortical thickness in the elderly. *Neuroimage* **52**,

780   1667–1676 (2010).

781   62. de Lange, A.-M. G. *et al.* White matter integrity as a marker for cognitive plasticity in aging.

782   *Neurobiol. Aging* **47**, 74–82 (2016).

783   63. Folstein, M. F., Folstein, S. E. & McHugh, P. R. 'Mini-mental state'. A practical method for grading

784   the cognitive state of patients for the clinician. *J Psychiatr Res* **12**, 189–198 (1975).

785   64. Beck, A. & Steer, R. *Beck depression inventory scoring manual*. (Psychologi. ed New York:

786   Psychological., 1987).

787   65. Salum, G. A. *et al.* High risk cohort study for psychiatric disorders in childhood: rationale, design,

788   methods and preliminary results. *Int J Methods Psychiatr Res* **24**, 58–73 (2015).

789   66. Pausova, Z. *et al.* Cohort Profile: The Saguenay Youth Study (SYS). *Int J Epidemiol* **46**, e19 (2017).

790   67. Ellis, K. A. *et al.* The Australian Imaging, Biomarkers and Lifestyle (AIBL) study of aging:

791   methodology and baseline characteristics of 1112 individuals recruited for a longitudinal study

792   of Alzheimer's disease. *Int Psychogeriatr* **21**, 672–687 (2009).

793   68. Mueller, S. G. *et al.* The Alzheimer's disease neuroimaging initiative. *Neuroimaging Clin. N. Am.*

794   **15**, 869–877, xi–xii (2005).

795   69. Reuter, M., Schmansky, N. J., Rosas, H. D. & Fischl, B. Within-subject template estimation for

796   unbiased longitudinal image analysis. *NeuroImage* **61**, 1402–1418 (2012).

797   70. Dale, A. M., Fischl, B. & Sereno, M. I. Cortical surface-based analysis. I. Segmentation and surface

798   reconstruction. *Neuroimage* **9**, 179–194 (1999).

799   71. Fischl, B., Sereno, M. I. & Dale, A. M. Cortical surface-based analysis. II: Inflation, flattening, and

800   a surface-based coordinate system. *Neuroimage* **9**, 195–207 (1999).

801   72. Fischl, B. & Dale, A. M. Measuring the thickness of the human cerebral cortex from magnetic

802   resonance images. *Proc. Natl. Acad. Sci. U.S.A.* **97**, 11050–11055 (2000).

803   73. Wood, S. N. *Generalized additive models: an introduction with R*. (Chapman Hall/CRC, 2006).

804   74. Fjell, A. M. *et al.* Critical ages in the life course of the adult brain: nonlinear subcortical aging.

805   *Neurobiol. Aging* **34**, 2239–2247 (2013).

806   75. French, L. & Paus, T. A FreeSurfer view of the cortical transcriptome generated from the Allen

807   Human Brain Atlas. *Front Neurosci* **9**, 323 (2015).

808   76. O'Leary, N. A. *et al.* Reference sequence (RefSeq) database at NCBI: current status, taxonomic

809   expansion, and functional annotation. *Nucleic Acids Res.* **44**, D733-745 (2016).

810   77. Wickham, H. *ggplot2: Elegant Graphics for Data Analysis*. (Springer International Publishing,

811   2016). doi:10.1007/978-3-319-24277-4.

812   78. Mowinckel, A. M. & Vidal-Piñeiro, D. Visualisation of Brain Statistics with R-packages ggseg and

813   ggseg3d. *arXiv:1912.08200 [stat]* (2019).

814   79. Douaud, G. *et al.* A common brain network links development, aging, and vulnerability to

815   disease. *PNAS* **111**, 17648–17653 (2014).

816   80. Vidal-Piñeiro, D. *et al.* The functional foundations of episodic memory remain stable throughout

817   the lifespan. *bioRxiv* 2020.01.30.926469 (2020) doi:10.1101/2020.01.30.926469.

818   81. Glasser, M. F. *et al.* The minimal preprocessing pipelines for the Human Connectome Project.

819   *Neuroimage* **80**, 105–124 (2013).

820   82. Huntenburg, J. M. *et al.* A Systematic Relationship Between Functional Connectivity and

821   Intracortical Myelin in the Human Cerebral Cortex. *Cereb. Cortex* **27**, 981–997 (2017).

822   83. Grydeland, H. *et al.* Waves of Maturation and Senescence in Micro-structural MRI Markers of

823   Human Cortical Myelination over the Lifespan. *Cereb Cortex* **29**, 1369–1381 (2019).

824   84. Colantuoni, C. *et al.* Temporal dynamics and genetic control of transcription in the human

825   prefrontal cortex. *Nature* **478**, 519–523 (2011).

826   85. GTEx Consortium. Human genomics. The Genotype-Tissue Expression (GTEx) pilot analysis:

827   multitissue gene regulation in humans. *Science* **348**, 648–660 (2015).

828   86. Trabzuni, D. *et al.* Quality control parameters on a large dataset of regionally dissected human

829   control brains for whole genome expression studies. *J. Neurochem.* **119**, 275–282 (2011).

830   87. Jaffe, A. E. *et al.* Mapping DNA methylation across development, genotype and schizophrenia in

831   the human frontal cortex. *Nat. Neurosci.* **19**, 40–47 (2016).

832   88. Piñero, J. *et al.* The DisGeNET knowledge platform for disease genomics: 2019 update. *Nucleic*

833   *Acids Res* **48**, D845–D855 (2020).

834